JOURNAL OF OPTOELECTRONICS AND ADVANCED MATERIALS Vol. 9, No. 12, December 2007, p. 3803 - 3807

Anomalous UV-Induced absorption spectra in the Rf-sputered In_2O_3-Sn polycrystalline films

J. EBOTHE[a], R. MIEDZINSKI[*], I. FUKS-JANCZAREK, A. H. RESHAK
[d]*Universite de Reims, Laboratoire LTME, France*
J.Dlugosz University, Czestochowa, Poland

Photoinduced absorption of the rf-sputtered indium tin oxide (ITO) thin films doped Sn in concentrations – 2, 4, 5, 6 and 10 % (in weighting units) is studied. We perform photoinducing treatment of the In_2O_3-Sn films by 1 ns nitrogen laser (λ=337 nm) during illumination up to 10 min. The absorption spectral maximum at 450 nm for the 1 m film samples possessing 2 % and 4 % of Sn is spectrally shifted up to 525 nm for 5 % Sn content. Moreover for 6 % of the Sn one can see an occurrence of the flat absorption maximum, at about 620 nm – 750 nm. With the further increase of the Sn content (up to 10 %) the spectrum becomes similar to that one for 2 % Sn samples. It is established a large spectral shift of the photoinduced absorption band at 500 nm for 2 % Sn content up to 540 nm for the 4 % Sn samples. However, a value of the total absorption changes is almost two times lower. This process is continued for the contents of 5 % and 6 % of Sn. A sign of the photoinduced absorption is changed up to opposite sign for the wavelengths higher than 650 nm. So we observe a phtobleaching. Explanation of the observed non-monotonical content-dependent photoinduced absorption is given within a framework of existed band energy calculations, particularly due to photoinduced shift of the Fermi energy. It is crucial that the effect is observed only for the films deposited by rf-sputtering and is not observed for the films grown by MOCVD, laser plasma ablation and spray pyrolysis. So the role of deposition conditions determining the film properties is crucial. Moreover, excitation by the wavelengths up to 2 μm do not show substantial changes, indicating on an absence of contribution of plasmon states.

(Received August 5, 2007; accepted December 2, 2007)

Keywords: In_2O_3, ITO-Sn, Optical absorption

1. Introduction

The synthesis and characterization of metal doped In_2O_3 films and nanocrystals have been studied intensively by many researchers [1,2]. There are a lot of researches devoted to their synthesis [3], conductivity [4], or crystal structure [5]. The above properties come in handy with regard on possibility of use in electronics devices such how flat panel displays, organic light emitting diodes and also solar cells. In this work we focus on UV-induced optical properties of Sn doped ITO. There were also reports about photoinduced optical and non-linear optical effects [6]. Particularly, it was shown principal role of the nanointerfaces separating the films and the glass substrates in the effects. Because the films mentioned were grown by spray pyrolysis method which do not have sufficient adhesion with the substrate it is difficult to perform the reliable analysis of the physical processes on the interfaces under the high power laser illumination. To receive more important results it would be good to have the samples possessing better adhesion with the substrates. As a consequence in the present work we will present investigations of the photoinduced absorption in the In_2O_3 films doped by different amount of Sn (2 %, 4 %, 5 %, 6 %, 8 %, 10 %) using radio-frequency sputtering method. Following the existed band energy structure calculations [7] such changes should lead to substantial shift of the Fermi energy. Using the nanosecond laser pulses hitting to the maximum of the electronic density of states one can vary substantially photo carrier occupation dynamics. Particularly one can shift the occupation of the trapping levels. For the investigated films more appropriate seems to be nitrogen laser generating at 337 nm.

2. Experiment

2.1 Crystallographic data of indium oxide

The indium oxide (In_2O_3) is a body centered cubic crystal, dimensions of the unit cell are a = b = c = 10.117 Å and contains 32 of indium atoms and 48 of oxygen atoms [8]. The space group is Ia3. In table 1 we shown all the atoms position in unit cell. The coordinates from table 1 we used to drew the unit cell of In_2O_3 crystal (Fig. 1.) in four different (hkl) orientations: (100), (010), (001) and (111).

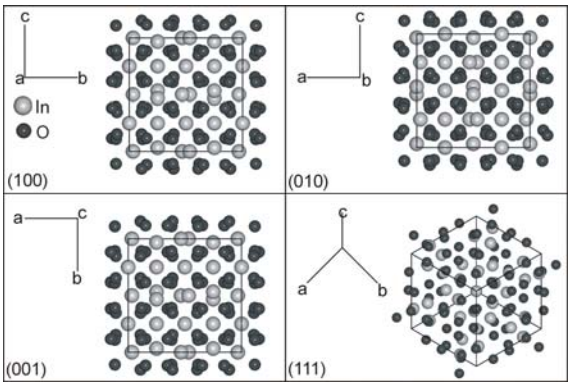

Fig. 1. The In_2O_3 crystalline structure.

Table. 1. The indium oxide atoms positions in unit cell.

o.	Atom	Coordinates [Å]			No.	Atom	Coordinates [Å]		
		x	y	z			x	y	z
1	Indium	2.5293	2.5293	2.5293	41	Oxygen	-3.8748	-3.9558	-1.5479
2	Indium	-2.5293	-2.5293	-2.5293	42	Oxygen	1.1837	1.1028	3.5106
3	Indium	-2.5293	2.5293	2.5293	43	Oxygen	-3.5106	1.1837	-3.9558
4	Indium	2.5293	-2.5293	-2.5293	44	Oxygen	1.5479	-3.8748	1.1028
5	Indium	-2.5293	-2.5293	2.5293	45	Oxygen	-1.5479	1.1837	3.9558
6	Indium	2.5293	2.5293	-2.5293	46	Oxygen	3.5106	-3.8748	-1.1028
7	Indium	-2.5293	2.5293	-2.5293	47	Oxygen	3.5106	3.8748	-3.9558
8	Indium	2.5293	-2.5293	2.5293	48	Oxygen	-1.5479	-1.1837	1.1028
9	Indium	4.7246	0.0000	2.5293	49	Oxygen	1.5479	3.8748	3.9558
10	Indium	-0.3339	-5.0585	-2.5293	50	Oxygen	-3.5106	-1.1837	-1.1028
11	Indium	-2.5293	4.7246	-5.0585	51	Oxygen	3.9558	3.5106	-1.1837
12	Indium	2.5293	-0.3339	0.0000	52	Oxygen	-1.1028	-1.5479	3.8748
13	Indium	-2.5293	-4.7246	0.0000	53	Oxygen	-3.9558	1.5479	-1.1837
14	Indium	2.5293	0.3339	-5.0585	54	Oxygen	1.1028	-3.5106	3.8748
15	Indium	-5.0585	2.5293	-4.7246	55	Oxygen	3.9558	-3.5106	-3.8748
16	Indium	0.0000	-2.5293	0.3339	56	Oxygen	-1.1028	1.5479	1.1837
17	Indium	0.0000	2.5293	4.7246	57	Oxygen	-3.9558	-1.5479	-3.8748
18	Indium	-5.0585	-2.5293	-0.3339	58	Oxygen	1.1028	3.5106	1.1837
19	Indium	4.7246	-5.0585	-2.5293	59	Oxygen	1.1837	-3.9760	-3.5106
20	Indium	-0.3339	0.0000	2.5293	60	Oxygen	-3.8748	1.1028	1.5479
21	Indium	-4.7246	0.0000	-2.5293	61	Oxygen	1.1837	3.9558	-1.5479
22	Indium	0.3339	-5.0585	2.5293	62	Oxygen	-3.8748	-1.1028	3.5106
23	Indium	2.5293	-4.7246	-5.0585	63	Oxygen	3.8748	-3.9558	3.5106
24	Indium	-2.5293	0.3339	0.0000	64	Oxygen	-1.1837	1.1028	-1.5479
25	Indium	2.5293	4.7246	0.0000	65	Oxygen	3.8748	3.9558	1.5479
26	Indium	-2.5293	-0.3339	-5.0585	66	Oxygen	-1.1837	-1.1028	-3.5106
27	Indium	-5.0585	-2.5293	4.7246	67	Oxygen	3.5106	-1.1837	3.9558
28	Indium	0.0000	2.5293	-0.3339	68	Oxygen	-1.5479	3.8748	-1.1028
29	Indium	0.0000	-2.5293	-4.7246	69	Oxygen	1.5479	-1.1837	-3.9558
30	Indium	-5.0585	2.5293	0.3339	70	Oxygen	-3.5106	3.8748	1.1028
31	Indium	-4.7246	-5.0585	2.5293	71	Oxygen	-3.5106	-3.8748	3.9558
32	Indium	0.3339	0.0000	-2.5293	72	Oxygen	1.5479	1.1837	-1.1028
33	Oxygen	3.9558	1.5479	3.8748	73	Oxygen	-1.5479	-3.8748	-3.9558
34	Oxygen	-1.1028	-3.5106	-1.1837	74	Oxygen	3.5106	1.1837	1.1028
35	Oxygen	-1.1837	3.9558	3.5106	75	Oxygen	-3.9558	-3.5106	1.1837
36	Oxygen	3.8748	-1.1028	-1.5479	76	Oxygen	1.1028	1.5479	-3.8748
37	Oxygen	-1.1837	-3.9558	1.5479	77	Oxygen	3.9558	-1.5479	1.1837
38	Oxygen	3.8748	1.1028	-3.5106	78	Oxygen	-1.1028	3.5106	-3.8748
39	Oxygen	-3.8748	3.9558	-3.5106	79	Oxygen	-3.9558	3.5106	3.8748
40	Oxygen	1.1837	-1.1028	1.5479	80	Oxygen	1.1028	-1.5479	-1.1837

2.2. Film growth

The films have been deposited in modified VUP2 (USSR) chamber using r.f. diode-sputtering from 16 cm ceramic pellet. The vacuum in the chamber was equal to about 10^{-5} Torr. As a variation parameter we have used oxygen pressure. The particular pellet targets during 15 min were treated in the in the chosen oxygen-argon mixture. Generally the method was similar to that one described in the Ref. 8.

The temperature substrate temperature was stabilized at 402 °C, distance between the substrate and target was about 5.6 cm and sputter Ar fluence-flux was about 18 sccm. The admixture of oxygen to the Ar sputter-gas, q_{O2}, has been varied systematically. Glass substrates (15×15-

mm BK7 glass) were controlled by ellipsometry and XRD methods.

The film thickness was evaluated by DicTac profilometer (France) and was equal to about 1 micrometer.

2.3 Photoinduced set-up

Photoinduced absorption measurements include three principal steps. First one consists in the spectrophotometer absorption measurements before the illumination. The second one includes treatment by the 5 ns UV laser up to appearance of saturation. And the third one – are the measurements of photoinduced absorption. A principal experimental schema is shown in Fig. 2. All of the ITO samples were irradiated by 10 minutes of pulsed nitrogen laser with repetition frequency about 7 Hz. The photoinducing laser had a wavelength 337 nm, a power 0.5MW pulse and pulse duration 5 ns. Spectrophotometric absorption spectra were measured by the Ocean Optics S1024DW spectrometer (spectral range 198 – 830 nm, spectral resolution 0.27 nm). The XRD diffraction control have shown that the films were polycrystalline ones and their morphological structure was equal to about 12 nm grains sizes. The measurements were performed following the spectral dependences of transmission spectra. After the absorption coefficients were evaluated by an equation:

$$K=1/d\ ln[(1-R)/2T+((1-R)^2/4T^2+R2)^{1/2}],$$

where d – is the film thickness; T and R correspond to the transmission and reflection coefficients, respectively. To eliminate an influence of interferometric effect the evaluation procedure was performed in more than 1200 different points.

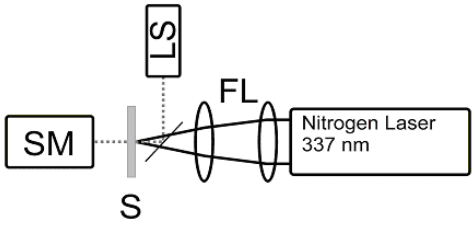

Fig. 2. The experimental setup: SM – spectrophotometer, S – sample, LS – white light source, FL – focusing lenses.

3. Results and discussion

In the Fig. 3-7 we present absorption spectra of the investigated samples before and after the illumination by nitrogen laser with parameters given above. Such parameters allow avoiding sample's overheating and corresponding annealing, which may drastically change the physical and structural properties [10]. Despite polarization of UV-induced light and probing beams influence the observed spectra. The illumination by the 10 min. UV-lasers causes a photo-saturated processes, however not the photochemical destruction and structural changes. This is a crucial fact, which is confirmed that the carrier density is changed only within the 10^{19} to 1.5×10^{20} cm^{-3}.

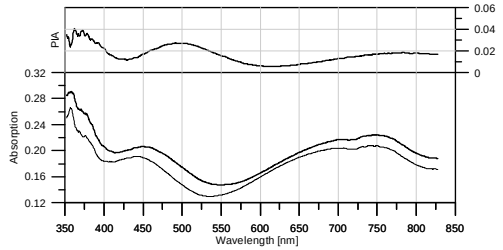

Fig. 3. Absorption spectra and photoinduced optical density of ITO with 2%-wt tin concentration. Bold line – spectrum before irradiated, thin line – spectrum after irradiated.

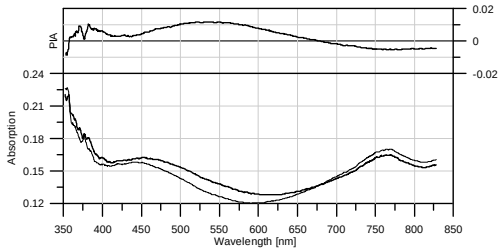

Fig. 4. Absorption spectra and photoinduced optical density of ITO with 4%-wt tin concentration. Bold line – spectrum before irradiation, thin line – spectrum after irradiation.

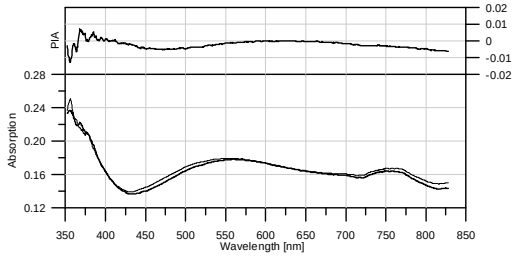

Fig. 5. Absorption spectra of ITO with 5%-wt tin concentration. Bold line – spectrum before irradiation, thin line – spectrum after irradiation.

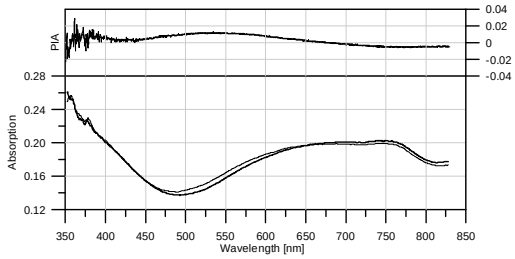

Fig. 6. Absorption spectra and photoinduced optical density of ITO with 6%-wt tin concentration. Bold line – spectrum before irradiation, thin line – spectrum after irradiation.

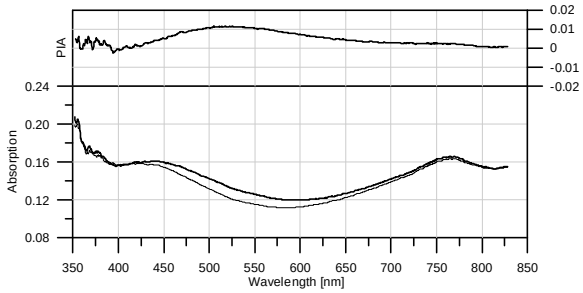

Fig. 7. Absorption spectra and photoinduced optical density of ITO with 10%-wt tin concentration. Bold line – spectrum before irradiation, thin line – spectrum after irradiation.

The obtained data (see Fig. 3 – Fig. 7) have shown that we observe a drastic influence of the UV-laser treatment on the absorption. We deal with two types of effects – the first one is related to substantial re-distribution of the Fermi energy under different photoinduced treatment of the carrier. The second one may be a consequence of catching the carriers by phonon trapping levels, which is efficient during the UV-treatment and role of the grain may be here crucial [11].

Comparing the Fig. 3 and Fig. 5 one can see that the absorption maximum at 450 nm for 2 % and 4 % doped Sn is shifted strongly up to 525 nm for 5 % Sn content. Moreover at 6 % of Sn one can see an occurrence of the flat wide spectral maximum, existing at about 620 nm – 750 nm. With the further increase of the Sn up to 10 % (see Fig. 7) the spectrum appears to be more similar to that one at the 2 % of Sn. Photoinduced changes give a large difference even between the 2 % and 4 % Sn doped samples (Fig. 3 and 4). Particularly, one can clearly see a long-range spectral shift of the photoinduced maximum at 500 nm for 2 % Sn specimens up to 540 nm for the samples with the 4 % Sn content. Simultaneously the value of the maximal absorption changes is almost twice less. This process is continued for the contents of 5 % and 6 % of Sn. Moreover the sign of the photoinduced absorption changes is varied for the wavelengths higher than 650 nm to the opposite sign. So we observe the photo bleaching. And similar to the general absorption 10 % Sn samples the observed photoinduced spectra are similar to the case of the 2 % Sn specimens.

Following the band energy calculations of the ITO-Sn compounds [7] one can conclude that the increasing Sn doping lead to occupation of two different principal site positions into the ITO single crystals. In1 (8b) and In2(24d). Following the band structure calculations these two positions form two different positions of the Fermi energy levels. So the observed content dependences may be a consequence of a competition between the local site position occupations.

It is crucial that the effect is absent for the films deposited by other techniques, like MOVCD, spray pyrolysis or laser ablation.

Illumination by the nitrogen pulsed laser at 337 nm hits directly to the spectral maximum of the electronic DOS [7,12]. So one can expect that due to the such photoexcitation we have an efficient pumping of the corresponding bands, which due to partial heating during the 10 min are trapped by the grain trapping levels possessing large electron-phonon interaction. So we observe an efficient photoinduced shift of the Fermi energy. The returning (reversible) process at 10 % may be caused by exhausting of the localized site positions and formation of the Sn aggregation, which may favor the process similar to the low content of Sn. Principal role in the observed effects play nano-confined states which form the flattered bands.

It is necessary to emphasize that illumination at wavelengths up to 2000 nm, corresponding to the plasma edges do not show any influence on the effect, which indicates on an absence of the effect doe to the plasmon edges and confirms a principal role of the UV-induced Fermi energy shift.

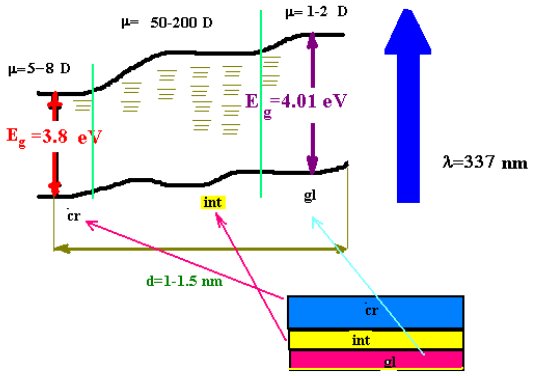

Fig. 8. Band energy mechanism of the photoinduced changes.

4. Conclusions

We performed photoinducing treatment of the rf-sputtered In_2O_3-Sn films by the 5 ns nitrogen laser at times up to 10 min. corresponding to the saturation of the photoinduced optical changes. The absorption maximum at 450 nm for 2 % and 4 % Sn doped samples is shifted drastically up to 525 nm at 5 % Sn content. Moreover at 6 % Sn content one can see an occurrence of the flat wide spectral maximum, which exists at about 620 nm – 750 nm. With the further increase of the Sn up to 10 % the spectrum appears to be more similar to that one at 2 % Sn content. Photoinducing changes give a large difference even between the 2 % and 4 % of Sn content contrary to absorption features. Particularly it was established a long-range spectral shift of the photoinduced maximum at 500 nm for 2 % Sn up to 540 nm for the samples with 4 % of Sn. Moreover the value of the maximal absorption changes is almost twice less. This process is continued for the contents 5 % and 6 %. Moreover the sign of the photo induced absorption changes is varied for the wavelengths higher than 650 nm up to the sign. So we observe the

phtobleaching. And similar to the general absorption at 10 % of Sn the observed photoinduced spectra are similar to the case of the 2 % Sn. Illumination by the nitrogen pulsed laser at 337 nm hits directly to the spectral maximum of the electronic DOS. Due to the such photoexcitation forming large number of photo carriers we have an efficient pumping of the corresponding bands, which due to partial photo pumping during the 10 min are trapped by the trapping levels possessing high electron-phonon interaction. The effect is absent for the films deposited by other techniques, like MOVCD, spray pyrolysis or laser ablation.

References

[1] Y. Xia, P. Yang, Y. Sun, Y. Wu, B. Mayers, B. Gates, Y. Yin, F. Kim, H. Yan, Adv. Mater. **15**, 353 (2003)

[2] C. N. R. Rao, F. L. Deepak, G. Gundiach, A. Govindaraj, Prog. Solid State Chem. **31**, 5 (2003).

[3] T. F. Stoica, M. Gartner, T. Stoica, M. Losurdo, V. S. Teodorescu, M. G. Blanchin, M. Zaharescu, J. Optoelectron. Adv. Mater., **7**(5), 2353 (2005).

[4] T. Kawashima, H. Matsui, N. Tanabe, Thin Solid Films **445**, 241 (2003).

[5] M. Kamei, H. Enomoto, I. Yasui, Thin Solid Films **392**, 265 (2001).

[6] I. V. Kityk, J. Ebothe, R. Miedzinski, M. Addou, H Sieder, A Karafiat, Semicond. Sci. Technol. **18**(6), 549 (2003).

[7] S. F. Matar, A. Villesuzanne, G. Campet, J. Portier, Y. Saikali, C. R. Acad. Sci. Paris, Chemistry **4**, 367 (2001).

[8] M. Marezio, Acta Cryst. **20**, 723 (1966).

[9] D. Mergel, M. Schenkel, M. Ghebre, M. Sulkowski, Thin Solid Films **392**, 91 (2001).

[10] L. Kerkache, A. Layadi, E. Dogheche, D. Remiens, J. Phys. D: Appl. Phys. **39**, 184 (2006).

[11] J. D. Mergel, Z. Qiao. J. Phys. D: Appl. Phys. **35**, 794 (2002).

[12] I. V. Kityk, J. Ebothe, A. ElHichou, B. ElIdrii, M. Addou, J. Krasowski. J. Opt. A: Pure Appl. Opt. **5**, 61 (2003).

[13] I. V. Kityk. Semicond. Sci. Technology. **18**(12), 1001(2003).

*Corresponding author: i.kityk@ajd.czest.pl